



End-to-end beam dynamics for CERN LINAC4

A.M. Lombardi, E. Sargsyan, S. Lanzone, J.B. Lallement, G. Bellodi, Maud Baylac, R. Duperrier, D. Uriot

► To cite this version:

A.M. Lombardi, E. Sargsyan, S. Lanzone, J.B. Lallement, G. Bellodi, et al.. End-to-end beam dynamics for CERN LINAC4. 39th ICFA Advanced Beam Dynamics Workshop High Intensity High Brightness Hadron Beams, May 2006, Tsukuba, Japan. pp.79-83. in2p3-00142207

HAL Id: in2p3-00142207

<https://hal.in2p3.fr/in2p3-00142207>

Submitted on 18 Apr 2007

HAL is a multi-disciplinary open access archive for the deposit and dissemination of scientific research documents, whether they are published or not. The documents may come from teaching and research institutions in France or abroad, or from public or private research centers.

L'archive ouverte pluridisciplinaire **HAL**, est destinée au dépôt et à la diffusion de documents scientifiques de niveau recherche, publiés ou non, émanant des établissements d'enseignement et de recherche français ou étrangers, des laboratoires publics ou privés.

END-TO-END BEAM DYNAMICS FOR CERN LINAC4

A. M. Lombardi, E.Z. Sargsyan, S. Lanzone, J.-B. Lallement, G. Bellodi, CERN, M. Baylac, LPSC Grenoble, R. Duperrier, D. Uriot CEA, Saclay.

Abstract

LINAC 4 is a normal conducting H^- linac which aims to intensify the proton flux available for the CERN accelerator complex. This injector is designed to accelerate a 65 mA beam of H^- ions up to 160 MeV for injection into the CERN Proton Synchrotron Booster. The acceleration is done in three stages : up to 3 MeV with a Radio Frequency Quadrupole (the IPHI RFQ) operating at 352 MHz, then continued to 90 MeV with drift-tube structures at 352 MHz (conventional Alvarez and Cell Coupled Drift Tube Linac) and, finally with a Side Coupled Linac at 704 MHz. The accelerator is completed by a chopper line at 3 MeV and a transport and matching line to the PS booster. After the overall layout was determined based on general consideration of beam dynamics and RF, a global optimisation based on end-to-end simulation has refined some design choices. The results and lessons learned from the end-to-end simulations are reported in this paper.

LINAC4 LAYOUT

The layout of LINAC4 is sketched in Figure 1. It consists of a RF volume source (identical to the one in DESY) which provides an H^- beam at 35 kV further post-accelerated to 95 keV. The first RF acceleration (from 95 keV to 3 MeV) is done by a Radio Frequency Quadrupole (the IPHI RFQ from CEA [1]). The RFQ resonates at 352 MHz, is 6 m long and it is powered by a 1 MW Klystron. At 3 MeV the beam enters a 3.6 meter long chopper line, consisting of 11 quadrupoles, 3 bunchers and two sets of deflecting plates. This system has the capability of removing micro-bunches on the RF scale and rematch the beam to the subsequent system of accelerators. A rudimentary collimation is also performed in this line. The beam is then further accelerated to 40 MeV in a conventional Drift Tube Linac at 352 MHz. The DTL, subdivided in 3 tanks, is 13.4 meters long and it is powered by 5 klystrons for a total power of 4 MW. Each of the 82 drift tubes is equipped with a Permanent Magnet Quadrupole. At 40 MeV the velocity of the beam is such as to allow the transition to structures which don't follow cell-by-cell the beam velocity profile. In LINAC4 the acceleration from 40 to 90 MeV is provided by a Cell-Coupled Drift Tube Linac at 352 MHz. The CCDTL is made of 24 tanks of 3 cells each for a total length of 25.3 meters. Three tanks are powered by the same klystron, for a total of 8 klystrons delivering 6.5 MW. The focusing is provided by electromagnetic quadrupoles placed outside

each tank. The acceleration from 90 to 160 MeV is done in a Side Coupled Linac resonating at 704 MHz. The SCL is made of 20 tanks of 11 cells each for a total of 28 m, powered by 4 klystrons delivering 12 MW. Focusing is provided by 20 Electromagnetic Quadrupoles.

This brings the total length of the linac to 80 m, for a total of 18 klystrons. The duty cycle of LINAC4 is 0.1% when used as injector to the PS booster but it grows to 3-4% if we consider its potential use as front-end of a high power proton driver like the SPL [2]. During the design phase we have decided to take as effective duty cycle the value of 15%: this value is used through the paper unless otherwise indicated.

END-TO-END SIMULATIONS

The H^- current from the source is 80 mA, reduced to 65 mA in each micro-pulse after the chopper line and 40 mA average in the pulse after chopping. The micro-bunch current, 65 mA, is such that space-charge effects are dominating at low energy and therefore some beam degradation can be expected. In particular the unavoidable transition to a slow phase advance in the chopper line (1 FODO per $10\beta\lambda$) is the weakest point as far as emittance growth and halo development is concerned.

After an initial phase of optimization of each section standalone to produce the layout of the accelerator, a campaign of end-to-end simulations with the purpose of identifying bottlenecks, weak points, and acceptance limitations allowed a fine tuning of the layout. The codes PATH [3], TOUTATIS [4] and TRACEWIN [5] have been made read/write compatible for the purpose of tracking beam from the low energy to the high energy end without regenerating a distribution at any point along the line.

RFQ

The beam dynamics in the IPHI RFQ has been extensively presented in [6]. The RFQ is capable of accelerating with an efficiency of more than 99% a beam of currents from 20 to 100 mA with limited emittance growth. Simulations show that, also for a perfectly matched beam, halo develops in the RFQ at the level of 10^{-4} and that transverse emittance grows by 8% for a 70 mA beam. The emittance growth happens in the RFQ coupling gaps, placed every two meter along the structure. Figure 2 shows very clearly this effect.

The RFQ is a very good transmission channel and therefore it doesn't filter the halo (also coming from the

source) which must be dealt with in the transfer line at 3 MeV.

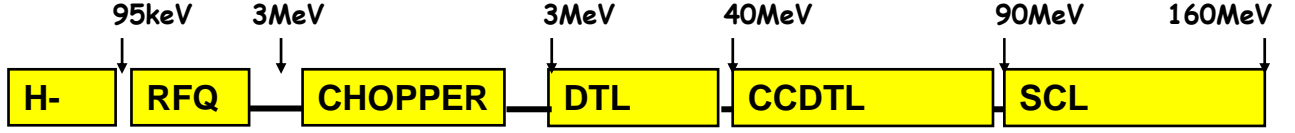


Figure 1 Schematic layout of LINAC4.

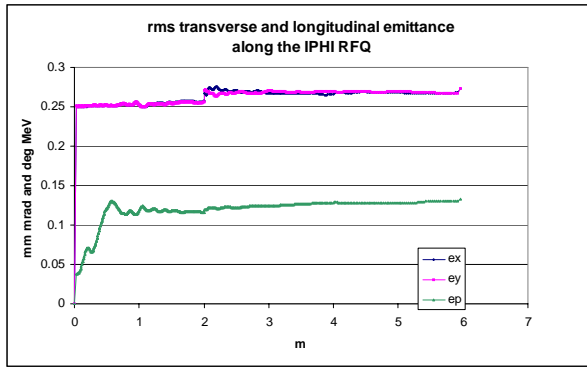


Figure 2 Transverse and longitudinal emittance along the IPHI RFQ.

Chopper Line

The chopper line houses a fast-switching electrostatic device able to remove 3/8 micro-bunches and a conical-shaped dump to dispose of the chopped micro-bunches. Both items are relatively bulky (the chopper is 800 mm long and the dump 120 mm) and therefore the focusing structure of the RFQ, one FODO period per $\beta\lambda$, i.e. 70 mm at 352 MHz and 3 MeV, must be interrupted. In order to keep the line compact and in order to break as little as possible the FODO structure, the chopper plates are mounted inside a quadrupole. In general all the elements are compacted to the maximum. The chopper plates are driven with an effective voltage of ± 400 V for a total deflection of 5.4 mrad. This allows separating the chopped and un-chopped beam at the output of the chopper plates in phase space but not in real space. The choice of the appropriate phase advance between chopper and dump allows for a separation in physical space at the dump position. The quadrupole between the chopper and the dump plays a key role in the process. Moreover this configuration minimises the voltage required from the chopper driver as the beam divergence in the chopper is minimised at the expenses of beam size. Unfortunately this trick entails some losses on the chopper plate, which are limited to 4% of the incoming beam, i.e. 1.3 kW. The picture of the transverse phase space of the chopped and unchopped beam at the output of the dump is shown in Figure 3.

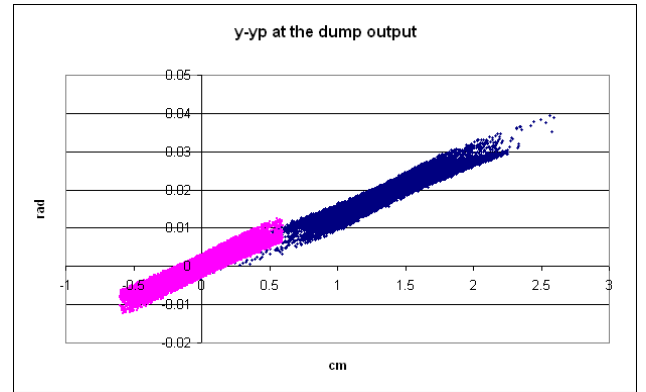


Figure 3 Transverse phase space of the chopped and unchopped beam at the dump.

Some 0.2% of the chopped beam is not stopped at the dump. This beam populates bunches that are supposed to be empty but it fits inside the transverse acceptance of the accelerator and it is therefore transmitted up to the high energy end. After the measurement campaign of 2008, which should confirm the presence of these unwanted particles, provision for eliminating them at the lowest possible energy should be studied [7].

After the dump, where the unwanted bunches have been disposed of, the beam is matched to the DTL focusing structure, which is a FFDD system in the first tank. Space-charge induced emittance growth is very severe when the beam is compressed back in volume to fit a fast phase advance focusing channel. In our case it amounts to almost 20 %.

DTL –CCDTL and SCL

After the operation of chopping, the beam is accelerated to 40 MeV in three DTL tanks equipped with Permanent Magnets. In the first tank the reference focusing scheme is FFDD whereas in the following tanks FODO is preferred. The reason for this choice is purely technical as it was not sure whereas the higher integrated gradient needed for a FODO at 3 MeV and 352 MHz was reliably achievable. The transition between the two focusing schemes is smooth and no emittance growth is observed provided the matching is done adequately.

The DTL is fully equipped with Permanent Magnet Quadrupoles, i.e. there isn't any possibility of adjustment at a later stage. We have verified that with the chosen

quadrupole settings,- optimised for 65 mA - currents in the range 20 mA to 70 mA could be accepted and that the electromagnetic quadrupoles in the chopper line could match the beam for the varying conditions.

At 40 MeV the beam is energetic enough to allow the transition to a structure which doesn't follow the beam velocity profile cell-by-cell. Acceleration to 90 MeV happens in a CCDTL composed of 3-gap tanklets. The average phase in each tanklet is -20 degrees and the focusing period is $3\beta\lambda$. At 90 MeV the structure employed is a SCL with 11 cells per tank. The variation of longitudinal phase advance due to the frequency jump at 90 MeV is controlled by adjusting the phase in the modules at the transition. The resulting phase advances are varying smoothly and do not give rise to emittance growth. Figure 4, Figure 5 and Figure 6 show the relevant parameters.

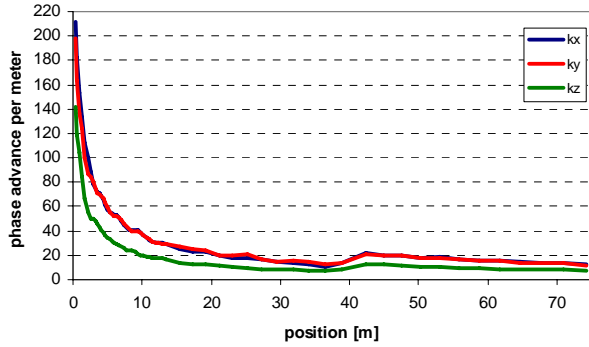


Figure 4 Full current phase advance per meter along the DTL-CCDTL-SCL.

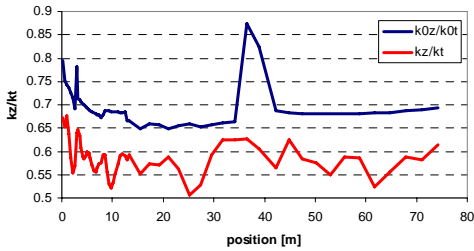


Figure 5 Longitudinal to transverse phase advance ratio along the DTL-CCDTL-SCL. Zero current (top) and full current (bottom).

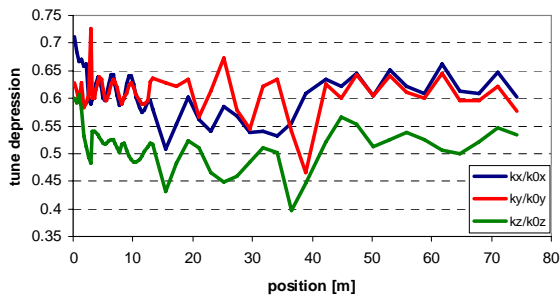


Figure 6 Tune depressions in the three planes along the DTL-CCDTL-SCL.

Towards the booster

At 160 MeV the beam phase space looks like in Figure 7. It presents some halo, which is very well transmitted throughout the machine and the energy spread must be reduced to match the acceptance of the PS booster. The extra complication in the design of this part arises from the difficulty of integrating the transfer line in the complex of CERN accelerators. Existing buildings and other accelerators make it necessary to have the line split in three sections with bending magnets in between. The most critical part from the beam dynamics point of view is the initial part, just after the SCL, where the beam has a big energy spread, and it is very compressed in phase. The combination of dispersion and space charge effects are difficult to handle without allowing for some emittance growth. The evolution of the emittance along the first part of the line is shown in Figure 8 : the effect of the dispersion, only partly compensated by the following bending is clearly visible.

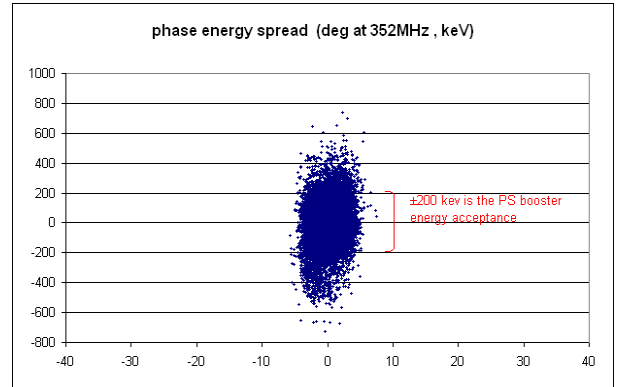
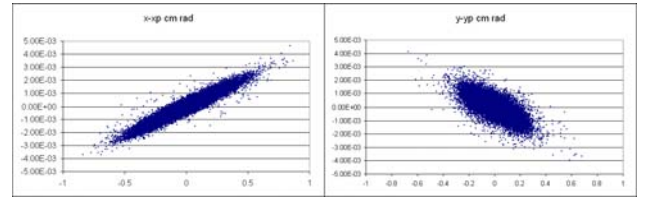


Figure 7 Beam phase space at the exit of the SCL: transverse planes (top) and longitudinal plane (bottom).

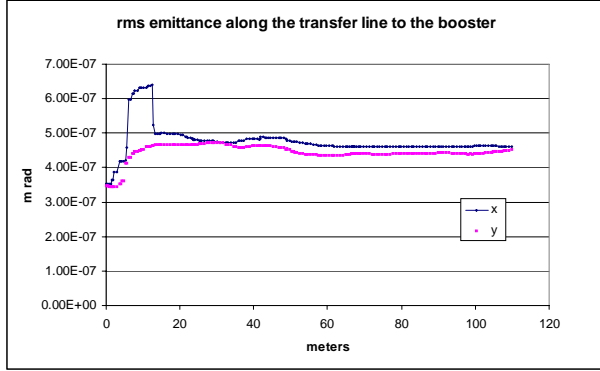


Figure 8 Transverse emittance along the 160 MeV transfer line.

Chopper-DTL-CCDTL-SCL

The IPHI-RFQ has been designed several years ago and it is now in the phase of manufacturing, therefore during the end-to-end simulation the output distribution of the RFQ has been taken as a fixed distribution as modification to the hardware were not possible anymore. In this section we present the results of the simulations from 3 MeV to 160 MeV.

The evolution of the rms emittance in the three planes as calculated with TRACEWIN and PATH are presented in Figure 9. The two codes have not been used, on purpose, in the same conditions: the space charge is computed with a 2D model in PATH and a 3D model in TRACEWIN. The maximum difference in the emittance is less than 10% and this gives us an idea of the accuracy of our calculations. When the two programs are run in the same conditions, the results differ by fraction of percent [8]. Besides the code comparison considerations, another important information can be gathered from Figure 9 : the majority of the emittance growth happens in the chopper line (3.6 meters) and just few percent in the rest of the accelerator (70 meters). This situation was foreseen and it is unavoidable as explained beforehand.

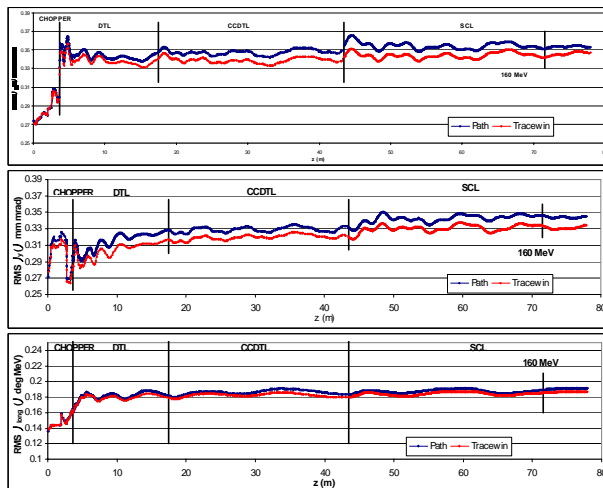


Figure 9 Rms emittance from 3 to 160 MeV. From top to bottom: x-xp; y-yp and longitudinal.

A quality factor of the solidity of the design is the ratio of the rms beam size to the radius of the vacuum chamber. In Figure 10 it is possible to see that the transverse bottleneck of LINAC4 is the chopper and the dump, where the aperture approaches the 2 rms beam size. Losses are localised in this area and the geometry of the chopper defines the minimum transverse acceptance of the whole LINAC.

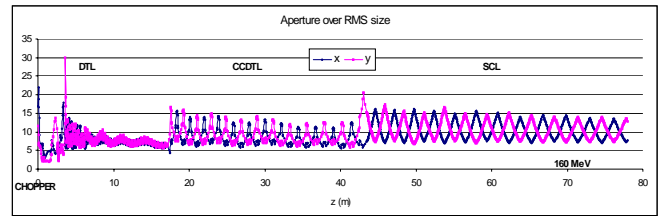


Figure 10 Aperture over the rms size along the chopper-DTL-CCDTL-SCL.

The equivalent acceptance in the longitudinal plane is difficult to define as the concept of “longitudinal losses” is less clearly defined than the transverse one. Nonetheless we have identified the bottlenecks or weak points in the longitudinal plane by comparing the phase and energy extension of the linearised bucket with the rms phase and energy extension of the beam. The expression used for the linearised bucket is the following:

$$\Delta\varphi = \pm \frac{3\varphi_s}{2}$$

$$\Delta W = \pm 2 \left[\frac{qmc^3 \beta^3 \gamma^3 E_0 T (\varphi_s \cos \varphi_s - \sin \varphi_s)}{\omega} \right]^{\frac{1}{2}}$$

where φ_s is the synchronous phase, β and γ the relativistic parameters, q the charge, m the mass, c the velocity of light, $E_0 T$ the effective accelerating field and ω the RF frequency.

Figure 11 shows the ratio of the two quantities above to the r.m.s. phase and energy spread of the beam. In LINAC4 the bottleneck for energy acceptance is the DTL input whereas the bottleneck for phase acceptance is the SCL input where there is a frequency jump of a factor of two. In the design of LINAC4 we have not respected the continuity of longitudinal acceptance at the transition between 352 and 704 MHz but we don't see degradation of performance also in presence of machine errors (RF amplitude and phase) [9].

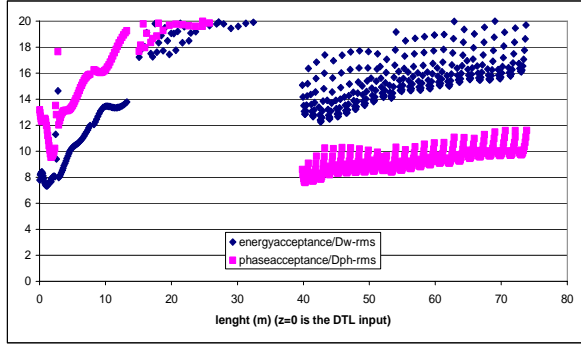


Figure 11 Ratio of the linearised bucket size to the rms phase and energy spread of the beam.

EMITTANCE BUDGET AND KNOWN BOTTLENECKS

Table 1 shows the rms normalised emittance and transmission along LINAC4. It is evident that most of the emittance growth and beam quality degradation happens before 3 MeV in the first stages of acceleration and during the chopping operations. The known causes of emittance growth are the energy spread from the source, the aberrations of the LEBT solenoids and the RFQ coupling gaps. The slow phase advance in the chopper line is another source of emittance growth as the beam grows 10 times its volume and it needs to be compressed back to be matched to the DTL. The emittance growth amounts to 75% from the source to 160 MeV, and it is acceptable for LINAC4 as injector to the booster as well as for its potential use as injector to a high power superconducting LINAC.

Table 1 Emittance along LINAC4

	95 keV (RFQ in)	3 MeV (DTL in)	160 MeV (SCL out)
Transverse emittance (rms mm mrad)	0.25	0.34	0.35
Longitudinal emittance (rms deg MeV)	0.13 (shaper)	0.17	0.18
Transmission		90%	90%
Current limit mA	20-70	20-70	20-70

Bottlenecks have been identified during the end-to-end simulation. The transverse emittance increase and transmission are defined in the chopper line and the only possible cure would be to have a higher chopper voltage. This in fact would allow for a larger distance between the plates and/or a shorter structure. The limit to the peak current per bunch (70 mA) comes from the first DTL cells. This bottleneck could be removed by adopting a FODO focusing system in the first tank.

The longitudinal acceptance is determined in the first cell of the DTL and the first cell of the SCL. This bottleneck could be removed if the LINAC4 were designed respecting the continuity of longitudinal acceptance, probably at the expenses of a longer machine. Longitudinal acceptance and current limit do not seem to be an issue, so these measures have not been implemented in the design.

LINAC4 VS. LINAC2

If LINAC4 is realised and put in operation as injector to the PS booster, it will substitute the present injector, LINAC2 [10].

Table 2 contains a comparison of the most important parameters of the two LINACs: the smaller emittance together with the higher energy and the possibility to charge-exchange at injection through a foil allow for a higher intensity and brilliance in the booster.

Table 2 comparison of LINAC2 and LINAC4

	LINAC2	LINAC4
Particle	protons	H ⁺
Energy	50 MeV	160 MeV
Current	160 mA	70 mA
Duty cycle	0.01%	0.08%
Erms,n	1.0mm mrad	0.4mm mrad

CONCLUSIONS

Linac4 is fit to inject into the CERN PS booster and improve its performance.

Linac4 is also ready to be the injector of a high power driver (4-5 MW) because the beam dynamics has been designed in view of mastering the losses at a higher energy; it is equipped with a chopper system at 3 MeV capable of removing micro-bunches at 352 MHz and all its components are designed for a 15% duty cycle.

REFERENCES

- [1] P.-Y. Beauvais, Recent evolutions in the design of the french high intensity proton injector (IPHI), Proc. European Particle Accelerator Conf., Lucerne, Switzerland, 2004.
- [2] F. Gerigk editor, Conceptual design of the SPL II, a high-power superconducting H- linac at CERN, CERN Report (CERN-2006-006)
- [3] A. Perrin, J.F. Amand, Travel v4.06, user manual, 2003.
- [4] R. Duperrier, N. Pichoff, D. Uriot, CEA Saclay codes review, ICCS Conference 2002, Amsterdam
- [5] R. Duperrier, "Toutatis, a radio-frequency quadrupole code", Phys. Rev. Spec. Top. Acc. & Beams, December 2000
- [6] R. Ferdinand, P.-Y. Beauvais, R. Duperrier, A. France, J. Gaiffier, J.-M. Lagniel, M. Painchault, F.

- Simoens, P. Balleyguier, "STATUS REPORT ON THE 5 MeV IPHI RFQ", proceeding of the XX LINAC conference, Monterey August 2000
- [7] JB Lallement, K. Hanke, M. Hori, A. M. Lombardi and E. Sargsyan , "Measurement strategy for the CERN Linac4 Chopper-line", these proceedings
- [8] J.B. Lallement, S. Lanzone, E. Sargsyan, "End-to-end simulations of LINAC4", AB-Note-2006-ABP.
- [9] M. Baylac, "Error study of LINAC 4 using transport code TraceWin , these proceedings.
- [10] D. J. Warner, "Accelerating structure of the CERN new 50 MeV linac" Proton Linear Accelerator Conference , Chalk River, Canada , 14 - 17 Sep 1976